water

MDPI

Article

Influence of Meander Confinement on Hydro-Morphodynamics of a Cohesive Meandering Channel

Parna Parsapour-Moghaddam * and Colin D. Rennie *

Department of Civil Engineering, University of Ottawa, 161 Louis Pasteur, Ottawa, ON K1N 6N5, Canada
* Correspondence: p.parsapour@uottawa.ca (P.P.-M.); Colin.Rennie@uottawa.ca (C.D.R.);
Tel: +1-613-562-5800 (ext. 6161) (P.P.-M.); +1-613-562-5800 (ext. 6124) (C.D.R.)

Received: 6 January 2018; Accepted: 19 March 2018; Published: 22 March 2018

Abstract: Despite several decades of intensive study of the morphological changes in meandering rivers, less attention has been paid to confined meanders. This paper studies the hydro-morphodynamics of two adjacent sub-reaches of a meandering creek, located in the City of Ottawa, Canada. Both of these sub-reaches are meandering channels with cohesive bed and banks, but one is confined by a railway embankment. Field reconnaissance revealed distinct differences in the morphological characteristics of the sub-reaches. To further study this, channel migration and morphological changes of the channel banks along each of these sub-reaches were analyzed by comparing the historical aerial photography (2004, 2014), light detection and ranging (LIDAR) data (2006), bathymetric data obtained from a total station survey (2014), and field examination. Moreover, two different spatially intensive acoustic Doppler current profiler (ADCP) surveys were conducted in the study area to find the linkage between the hydrodynamics and morphological changes in the two different sub-reaches. The unconfined sub-reach is shown to have a typical channel migration pattern with deposition on the inner bank and erosion on the outer bank of the meander bend. The confined sub-reach, on the other hand, experienced greater bank instabilities than the unconfined sub-reach. The average rate of bank retreat was 0.2 m/year in the confined sub-reach whereas it was lower (0.08 m/year) in the unconfined sampling reach. In the confined sub-reach, an irregular meandering pattern occurred by the evolution of a concave-bank bench, which was caused by reverse flow eddies. The sinuosity of the confined sub-reach decreased from 1.55 to 1.49 in the 10-year study period. The results of the present study demonstrate the physical mechanisms by which meander confinement can change the meandering pattern and morphological characteristics of a cohesive clay bed creek.

Keywords: meandering rivers; meander confinement; cohesive bed rivers; hydro-morphodynmics; spatial ADCP survey

1. Introduction

1.1. Background

Many river scientists and engineers have studied meandering rivers over the past few centuries (e.g., [1–16]). Despite the fact that river meandering is an erudite topic with a long literature history, there are still some uncertainties on the source and initiation of the meandering pattern and its migration. It is known that river meandering is associated with the bank erosion mechanism and can be influenced by the spatial progression of bars [17].

Bank instability and erosion are intrinsic characteristics of meandering rivers [18]. Lanzoni and Seminara illustrated how the morphodynamics of meandering rivers can be impacted by meander

instability [8]. River meandering may also lead to a flow separation which could impact bank erosion patterns [11,19–23]. Bank erosion processes influence a wide range of social, environmental and economic factors [24]. Consequently, bank erosion predictions are of essential importance in sustainable river management [25]. Despite numerous well-documented previous studies devoted to the bank retreat mechanism, the erosion of cohesive river substrates is not completely understood [26–28]. Cohesive properties of river banks can impact the rate of bank erosion [29]. Unlike non-cohesive river bed sediments for which resistance to entrainment is merely mechanical, cohesive material interactions depend on the electro-chemical bonds amongst the particles [26]. Furthermore, several studies have recognized the significance of pore water pressure in the erosion and removal of cohesive bed river particles or assemblages e.g., [30–33]. However, a general predictive theory for entrainment of cohesive river boundary sediments is yet to be developed; thus, prediction of bank erosion in a cohesive river remains challenging [27]. Bank erosion and subsequent meander migration are important natural processes for both unconfined and partially confined rivers [34].

Although meander morphodynamics have been widely studied, less attention has been paid to confined meandering. The morphological development of a confined meander is impeded by a natural or manmade restriction. A confined meander cannot freely develop, which results in a distinctive meander pattern that differs from those presented by freely meandering rivers. Nicoll noted that the dynamics of meander migration may be affected in confined meandering rivers [35], and Ghinassi et al. observed that meander confinement can lead to the downstream migration of fluvial point bars [36].

Lewin and Brindle showed that free meandering could be hindered by bedrock or anthropogenic structures [37], and this can result in a square-wave shape meandering configuration. They defined three degrees of confinement: first-degree confinement takes place in wide valleys whereby the stream impinges irregularly against the confining valley wall. Lane called this type of meander a "restrained" meander [38]. In second-degree confinement, the outer side of each meander bend impinges upon the confining wall, and in third-degree confinement, the meandering stream does not have space to progress.

Most river meanders do not undergo purely downstream translation. Nicoll observed downstream translation without substantial distortion only in confined meanders with limited amplitude and low curvature [35]. Lewin and Brindle noted that downstream translation without meander deformation is prevalent in second-degree confined rivers [37]. Nicoll and Hickinstudied the planform geometry and migration pattern of several second-degree confined meandering rivers on the Canadian prairies [39]. They related the channel-migration rate of the studied rivers to basic geomorphic and hydrologic variables. The authors indicated that the planform relations were generally consistent with those manifested by freely meandering rivers, with small yet significant differences due to the distinctive meander behavior of confined meanders.

Previous studies have shown that meander confinement can lead to development of a concave-bank bench [40–44]. A concave-bank bench is a crescent-shaped accretion on the upstream portion of the outer bank (concave side) of a meander bend. These deposits are generally observed in meandering rivers that migrate down valley [45]; however, they may also occur in unconfined meander belts [41,44,46]. Page and Nanson demonstrated that when the channel flow has the power to erode the channel banks [41], regular meandering is developed with a point bar and overbank deposition. However, in cases where the stream power hardly surpasses the shear strength of the bank material, then irregular meanders may be generated with long straight reaches and sharp bends. They showed that concave-bank benches are commonly developed when sharp meander bends migrate downstream.

The effect of manmade features on meandering river morphodynamics has been studied, particularly for river stabilization works [47]. Nevertheless, less studied has been the morphodynamics of meandering rivers confined by structures such as railway and road embankments [37]. Furthermore, the migration behavior of confined bends has been studied, most previous research has focused on second-degree confinement where the river impinges against the confining edge in every meander wavelength [39].

1.2. Objectives and Structure

As outlined above, there are still some uncertainties on the source and initiation of the meandering pattern and its migration, particularly for cohesive bed rivers. Moreover, the morphology and dynamics of confined meandering rivers are relatively poorly studied. Due to natural or manmade restrictions, confined meanders cannot freely develop, and this makes them have a meander pattern distinct from those presented by freely meandering rivers. Previous studies of confined meandering rivers have been mostly limited to second-degree confinement. Moreover, to the best of our knowledge, the hydrodynamics of a confined meandering channel have not previously been studied in terms of measuring the spatial distribution of the velocity flow field. Given the prevalence of confined meandering rivers, enhancing the understanding of their behavior in the landscape is of essential and practical importance for sustainable river management.

In this study, we evaluate the meander migration dynamics in a first-degree confining medium, i.e., in which the river makes irregular contact against a confining railway embankment, in a meandering cohesive bed river. We employ a paired sub-reach study approach, wherein one sub-reach is freely meandering and the second adjacent sub-reach is first degree confined by the railway embankment. Morphodynamics of each sub-reach are measured by repeat surveying over a multi-year period. Specifically, channel migration and morphological changes of the channel banks along each of these sub-reaches are analyzed by comparing historical aerial photography, light detection and ranging (LIDAR) data and bathymetric data obtained from a total station survey. Furthermore, channel hydrodynamics are measured in both sub-reaches by spatially intensive acoustic Doppler current profiler (ADCP) surveying, which, to the best of our knowledge, has not previously been conducted in a confined meander. This allows for a direct comparison of the hydrodynamic characteristics of unconfined and confined sub-reaches. Furthermore, the measured velocity fields are used to find linkages between the channel hydrodynamics and morphological changes. We are thereby able to explore how local meander confinement leads to different hydro-morphodynamic characteristics and corresponding meander morphology. The methodology employed in this study is comprehensively explained in the next section (Section 2). Results are shown in Section 3, followed by the discussion (Section 4) and conclusions (Section 5).

2. Methodology

2.1. Study Site

Watts Creek flows into the Ottawa River at Shirley's Bay in the Kanata region of the City of Ottawa, Canada (Figure 1). Two upstream branches (Watts Creek and Kizell Drain) join at a confluence situated at 45.340172° latitude, −75.880610° longitude (UTM 431006 m E, 5021119 m N). Watts Creek has been recognized as providing important coolwater fish habitat [48]. Rates of channel degradation are still not clear. In this study, we mainly focus on two adjacent sub-reaches. The two sub-reaches are M3 and M4 (Figure 1c). Both of these sub-reaches are meandering channels with a cohesive bed and banks. M4 is partially confined by the City of Ottawa rail line, and thereby is undergoing enhanced erosion. Watts Creek is a semi-alluvial channel offering a diverse habitat, with a mixture of runs, pools, and riffles. While fine clay and silt substrate is prevalent in Watts Creek, some coarse gravel is also present. Watts Creek has a bed that consists of a high (>30%) percentage of clay, i.e., soil particles that are smaller than two to four micrometers [49]. Clay particle properties cannot be as straightforwardly predicted because cohesion is dictated by electrostatic forces, which depend on the chemical composition of the clay particles. In addition, the natural consolidation state and hydraulic conductivity, organic matter, and a few other properties influence particle cohesion. The results of the bed sediment core samples collected from the entire reach indicated that all median grain sizes were in the silt or clay range which characterized them as fine grained, cohesive soils. The results of a piston-flume critical bed shear stress test suggest that the cohesive clay bed sediments in Watts Creek watershed are not heavily consolidated.

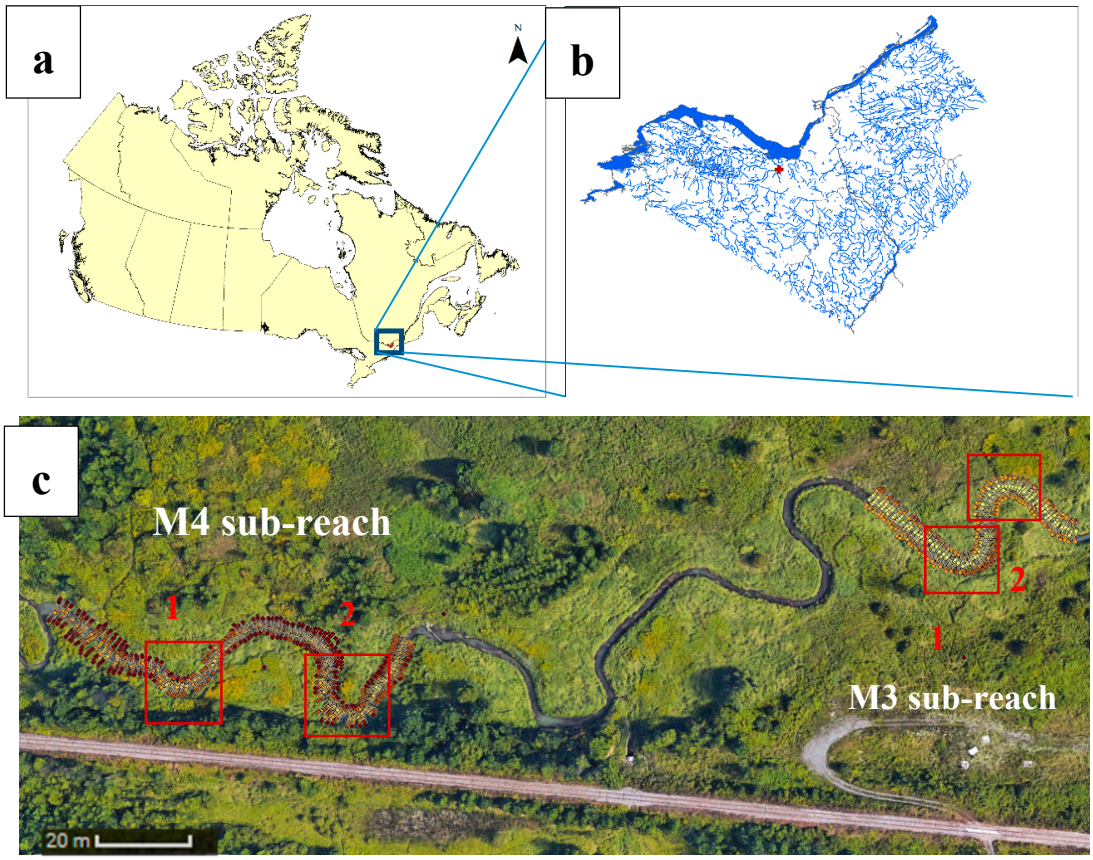

Figure 1. (**a**) Location of the study area within Canada (adopted from https://www12.statcan.gc.ca); (**b**) Study reach location in the Ottawa Study reach location in the Ottawa area (adopted from http://data.ottawa.ca/en/dataset/water); (**c**) Surveyed sections in Watts Creek sampling reaches M4 (to left) and M3 (to right) including total station surveyed points, flow from west (left) to east (right) (adopted from Google earth). Squares show the meander locations and their referred number within each sub-reach. Please note that the study area is situated at 45.340172° latitude, −75.880610° longitude.

2.2. Site Reconnaissance

Channel condition was assessed by visual observation during different flow regimes. The observations are categorized by location within each sampling sub-reach specified in Figure 1c. As is shown, M4 sub-reach of Watts Creek is confined by the City of Ottawa rail line. M3 and M4 are otherwise similar; they are meandering channels with cohesive bed and banks. They convey the same discharge (based on the ADCP measurements), and they have similar bed substrate and riparian vegetation. Figures 2–5 show the field conditions immediately after a spring freshet flood. Locations of erosion and channel incision were identified by exposed tree roots and steep, undercut or collapsing river banks. Observations for each sampling reach are provided below.

2.2.1. M4 Sampling Reach

This part of Watts Creek meanders is adjacent to the City of Ottawa rail line. Overbank sediment deposits throughout this reach indicated that the previous spring freshet had overtopped the banks in the Main Creek. Figure 2a shows the development of a concave-bank bench on the upstream limb of the outer bend at the last sharp meander. There were indications of instabilities on the downstream portion of the outer bends in M4 (Figure 2b). Inner bank instability was also observed at the upstream bend in M4. As shown in Figure 3a, an erosion pathway cut through the inner bank point bar during the freshet flow; vertical stakes in the channel suggest failure of a previous attempt to stabilize the

inner bank (Figure 3b). Figure 4a illustrates the evolution of the longitudinal-shaped bar as well as the secondary channel adjacent to the outer bank of the last meander bend. These features suggest that M4 has a very active, unstable channel, presumably due to the meander confinement by the rail line.

Figure 2. M4 sampling reach, meander bend restrained by the City of Ottawa rail, facing downstream. Note the City of Ottawa rail line immediately adjacent to the south of the river: (**a**) Concave-bank bench formation on the upstream of the bend apex; (**b**) The failure of outer bank, downstream of the bend apex. Pictures were taken by the authors on 30 April 2014.

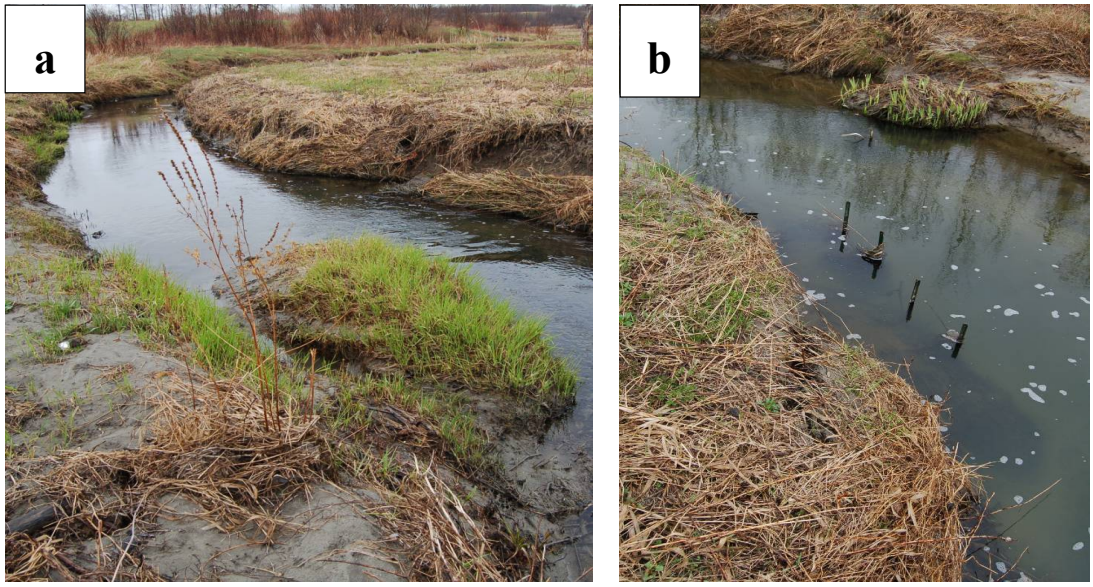

Figure 3. M4 sampling reach, meander bend restrained by the City of Ottawa rail, facing downstream: (**a**) Inner bank was overtopped during the previous high freshet flow, to an erosion pathway through the inner bank; (**b**) Vertical metal stakes used for bank stabilization. Pictures were taken by the authors on 30 April 2014.

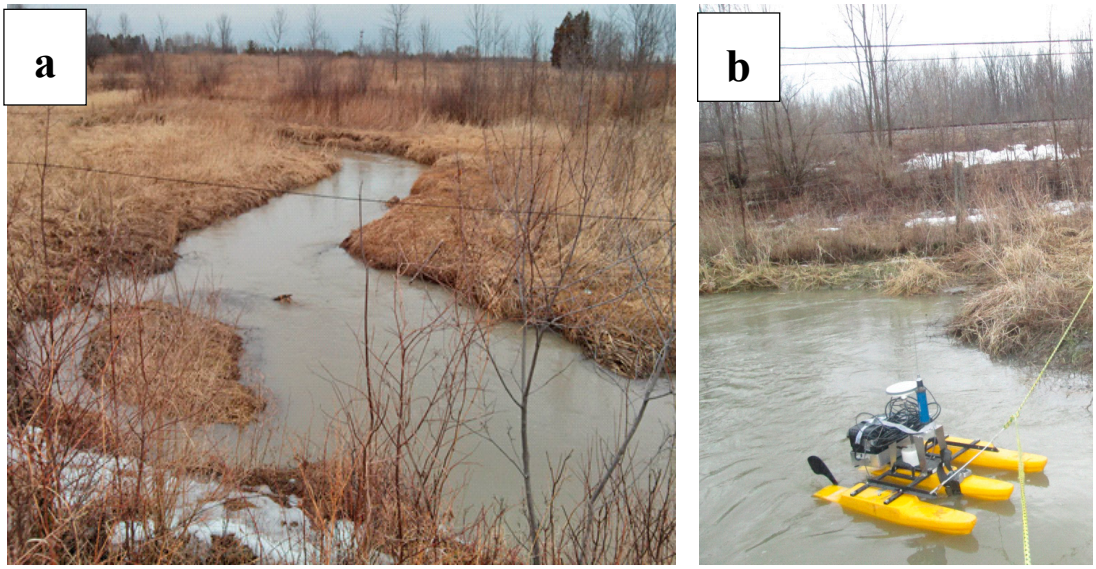

Figure 4. M4 sampling reach: (**a**) meander bend restrained by the City of Ottawa rail, facing upstream. Formation of the longitudinal bar and the secondary channel on the upstream of the outer bend apex; (**b**) ADCP spatial survey in the study reach. The City of Ottawa rail line can be seen immediately adjacent to the south of the river. Pictures were taken by the authors on 14 April 2015.

2.2.2. M3 Sampling Reach

Sampling reach M3 encompasses two unconfined meander bends. The channel is reasonably stable in M3, displaying only modest bank slumping on the outer bank downstream of a bend apex. This unconfined section of the creek represents a regular meandering pattern with moderate erosion on the outer bank and deposition on the inner bend (Figure 5b).

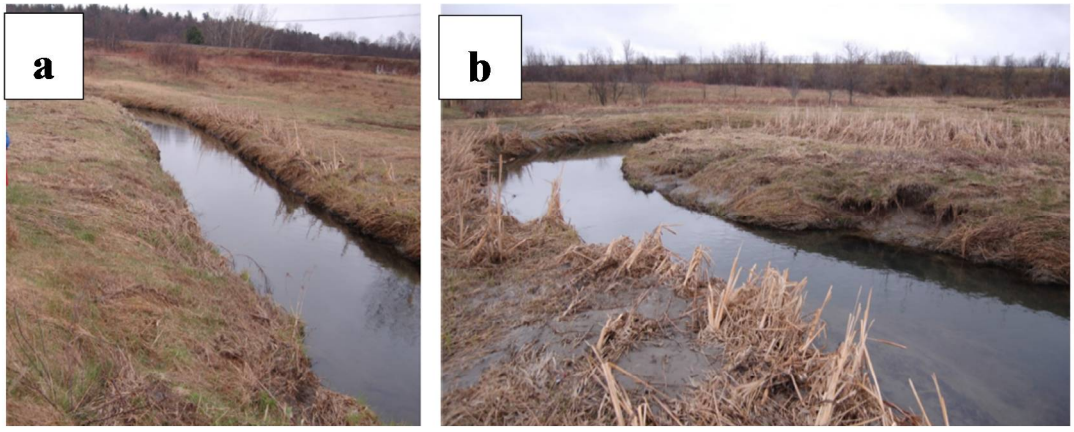

Figure 5. M3 facing downstream: (**a**) In the middle of M3, between the two major bends; (**b**) Last meander bend manifests regular meandering pattern with erosion on the outer band and deposition in the inner bank. Pictures were taken by the authors on 30 April 2014.

2.3. Data Collection and Analysis

Morphological studies of the two sub-reaches were done based on the results of: (a) bathymetric survey of each section (b) available LIDAR data (c) historical aerial photographs. A topographic and bathymetric study was conducted during summer 2014, employing a total station survey to accurately distinguish the bank and bed topography. Over 4065 bathymetric points were collected in both study sub-reaches with an average spacing of 1.2 and 0.3 m in streamwise and cross-stream directions,

respectively (Figure 1c). The collected points were then interpolated by the TIN interpolation method in ArcGIS10.2 (Esri, Redlands, CA, USA) to obtain the DEM (Digital Elevation Model) of 2014. Slope and hillshade maps were then obtained from the DEM.

The expense of river hydro-morphological field studies has increased utilization of aerial survey techniques [50]. Relatively recent development of LIDAR technology allows for accurate measurements of bank locations and elevations [51]. The City of Ottawa has collected LIDAR data for various parts of the city during different years. This study employs available LIDAR data of the study creek from 2006 obtained from the National Capital Commission (NCC). We converted the LIDAR data to DEMs using ArcGIS. Historical aerial photographs were acquired using Google Earth. The photos were registered using georeferencing tools available in ArcGIS. Stationary ground control points for rectification were obtained using corners of the buildings, road intersections, rail trail, solitary trees and large rocks nearby the study site. Figure 6 shows the aerial images of the study reach from 2004 and 2014. It should be noted that both aerial photos show the site condition in the summer (June) which represents the low flow regime (discharge ~0.15 m^3/s based on 2014 ADCP measurements) in the study creek.

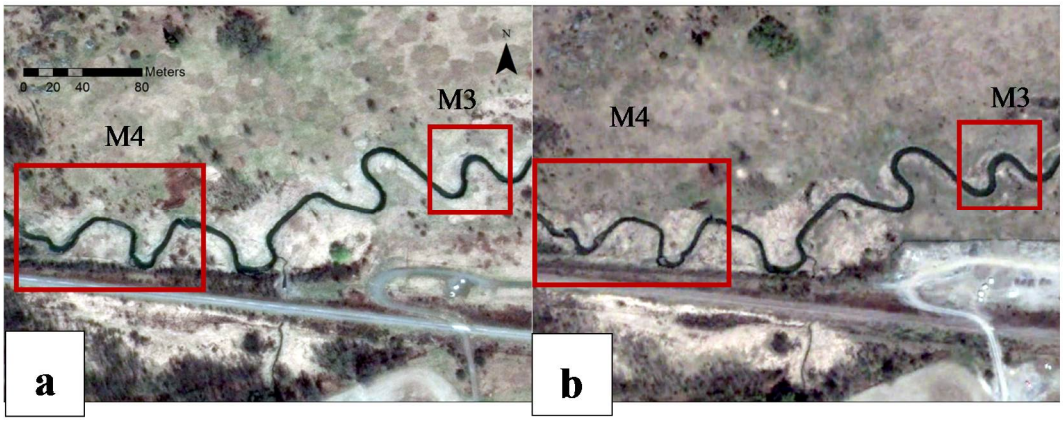

Figure 6. Aerial photo of the study reach adopted from Google Earth: (**a**) 2014 (**b**) 2004. Location of the each sampling reach is shown with the square.

A comparison was then made between the aerial photographs (2004 and 2014), DEMs obtained from the LIDAR data (2006) and total station surveys (2014). The river DEM maps from 2004, 2006 and 2014 were overlapped in ArcGIS, and polygons were created to define the active channel boundary and the bank retreat. To distinguish the location of the base and top of the river banks during different times, slope classification maps were overlapped with the hillshade maps for both LIDAR and surveyed DEMs. This allowed for assessment of the meander behavior and bank retreat of each sub-reach. Having DEMs of the study creek at different periods also allows for measurements of elevation changes. Accordingly, the DEM from 2006 was subtracted from that of 2014 through the raster calculator tool in ArcGIS to produce a DEM difference raster to explore the amount of erosion and deposition [52].

In order to evaluate the effect of the velocity field on the channel morphology, spatially intensive ADCP surveys were conducted in both study reaches during August (low flow) and October (moderate flow) 2014. According to the ADCP measurements, flow discharge was 0.17 and 0.45 m/s under low and moderate flow, respectively. It should be noted that the bankfull discharge was approximately 1.4 m/s [53], and the return flow of the high flow was estimated to be 1.4 years [54]. A Sontek M9 River Surveyor ADCP was deployed on an Ocean Sciences trimaran riverboat (Figure 4b). Standing on opposite banks of the creek, we operated the trimaran boat with ropes and moved the boat downstream in narrowly spaced transects in a zigzag array. The measured depth-averaged velocity data were then post processed using in-house Matlab codes [55]. Parsapour-Moghaddam and Rennie provide further details on conducting a spatially intensive ADCP survey in a clay-bed meandering river [16,56,57].

3. Results

Table 1 illustrates the channel and flow characteristics of both sub-reaches during ADCP measurements at the moderate flow in 2014. As can be seen, the channel and averaged values of the flow characteristics were quite similar in both sub-reaches.

Table 1. Channel and flow characteristics in the study area based on the ADCP measurements at the moderate flow in 2014.

Parameter	M4 Sub-Reach	M3 Sub-Reach
Channel slope	0.0017	0.0016
Averaged width (m)	3.4	3.6
Averaged depth (m)	0.4	0.6
Averaged discharge (m^3/s)	0.45	0.45
Averaged flow velocity (m/s)	0.2	0.17
Average Froude number	0.1	0.07

We compared the position of the active channel mapped from 2004 aerial photography with that of 2014. This is shown for both M4 and M3 sampling reaches in Figures 7 and 8, respectively. The boundaries were obtained through digitizing the channel margin based on the aerial images in ArcGIS. A sufficiently large number of vertices was employed to avoid digitization errors. Figure 9 shows the cumulative erosion and sedimentation that occurred in the channel margins between 2006 (based on the LIDAR data) and 2014 (based on the total station survey). This was obtained by subtracting the 2006 DEM of the study area from the corresponding 2014 DEM.

Figure 8 shows that the M3 sampling reach exhibited a typical meandering pattern in which erosion and deposition occur at the outer and inner bank, respectively. This can be seen in Figure 9b where negative and positive values show erosion (outer bend) and deposition (inner bend), respectively. This confirms our field observations (Figure 5). Table 2 illustrates that the sinuosity of this sub-reach was more-or-less consistent, with only a slight increase from 2004 to 2014.

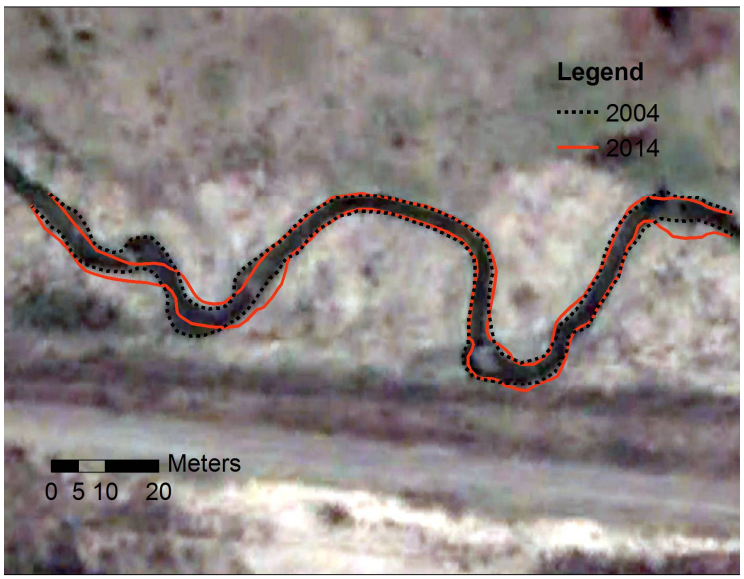

Figure 7. Channel margin migration along the M4 sampling reach. Flow from left (west) to right (east). Background image adopted from Google Earth image (2004).

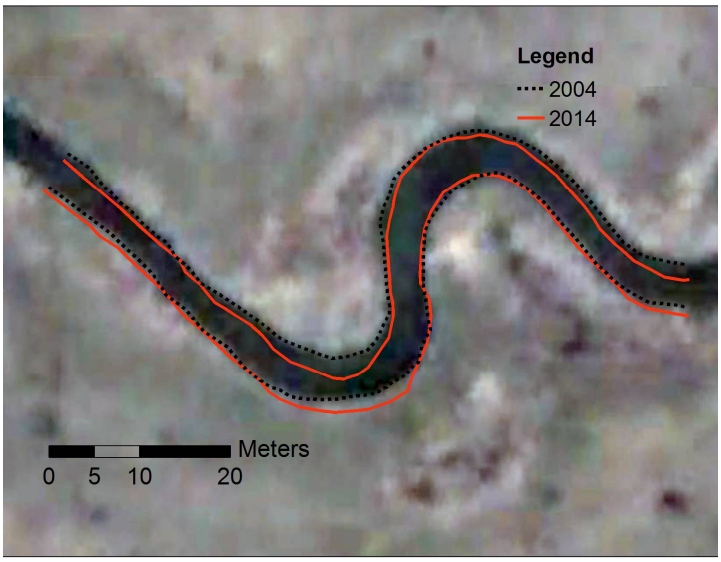

Figure 8. Channel margin migration along the M3 sampling reach. Flow from left (west) to right (east). Background image adopted form Google Earth image (2004).

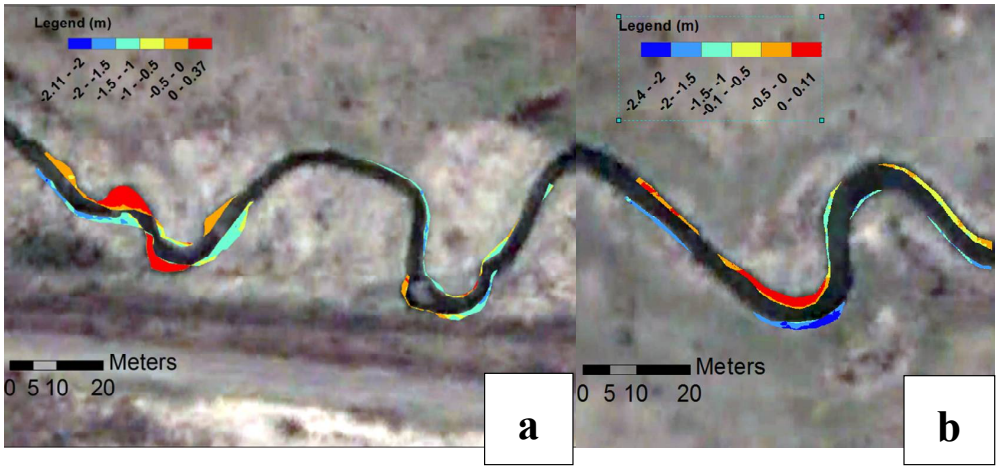

Figure 9. Erosion (negative) and deposition (positive) (m) from 2006 to 2014 in: (**a**) M4 and (**b**) M3 sampling reaches. Background image adopted form google earth image (2004).

Table 2. Channel geometry of each sub-reaches of the study creek within different years.

Sampling Reach	Date	Length of the Channel Path (m)	Sinuosity
M4	2004	187.88	1.55
	2014	175.27	1.49
M3	2004	106.26	1.44
	2014	107.1	1.46

On the contrary, the M4 sampling reach (Figure 7) showed irregular meandering behavior. From Table 2, it can be inferred that the sinuosity of the channel decreased from 1.55 to 1.49 in the 10-year period. As shown in both Figures 7 and 9a, a concave-bank bench can be observed in the upstream limb of the outer bank of the first meander bend. Furthermore, a longitudinal bar is developing in the second meander bend, which may be a precursor to concave bank bench. These results are consistent with the results of our field reconnaissance (Figures 2a and 4a). On the other hand, Figures 7 and 9a indicate the occurrence of bank erosion on the downstream of the outer bend apex at the confined meander bends.

This was also observed during the field site examination (Figure 2b). Apparently, the sharp meander bends of M4 sampling reach migrated downstream whereas the straight portion seemed to be more stable. The average rate of bank retreat in the M4 sub-reach was 0.2 m/year, while it was 0.08 m/year in the M3 sub-reach.

To study further the hydro-morphodynamics of the irregular meandering development observed in the confined sampling reach in the study creek, spatially distributed ADCP depth-averaged velocities were employed. Figures 10 and 11 show the interpolated measured depth-averaged velocities during both low flow and moderate flow in the meander bends of the M4 and M3 sub-reaches, respectively. As shown in Figure 10, reverse flow occurred in the confined meander bends while the unconfined meanders had a regular flow pattern in the streamwise direction (Figure 11). The reversing flow was associated with the irregular bend geometry and the flow obstruction imposed on the bend flow by the concave-bank bench.

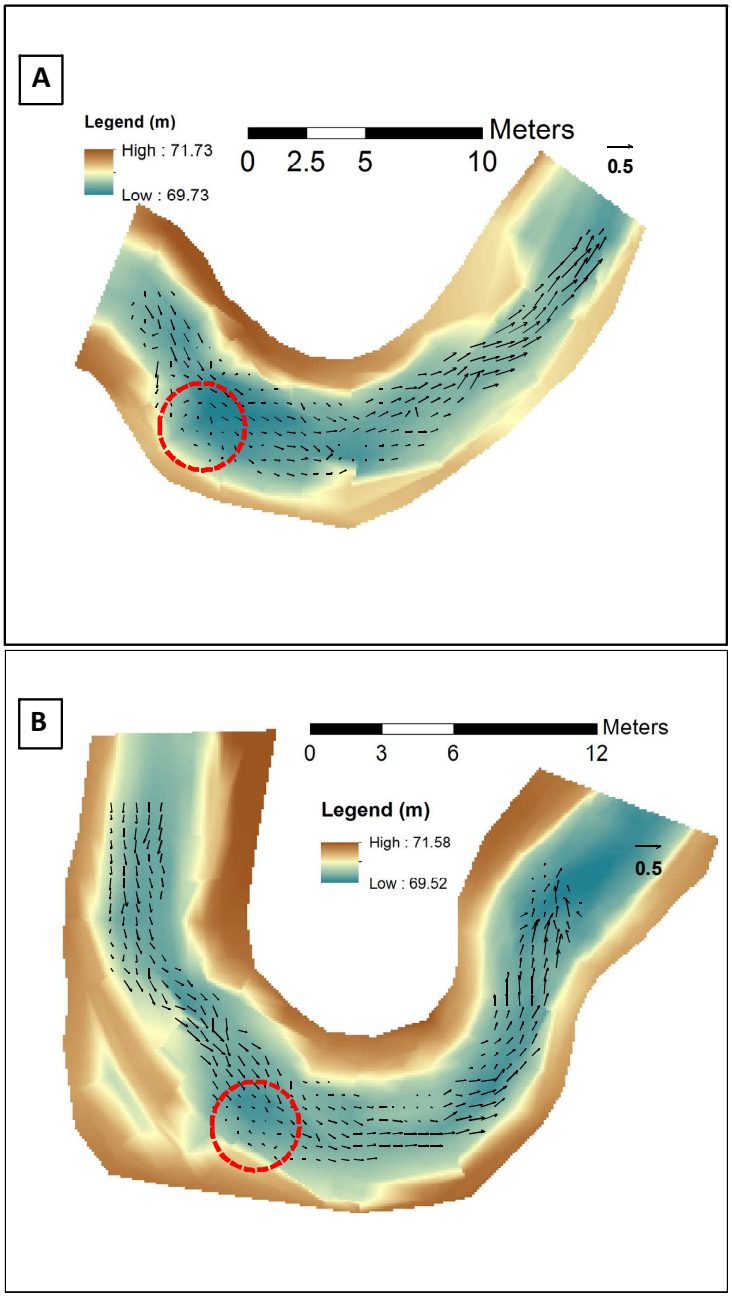

Figure 10. *Cont.*

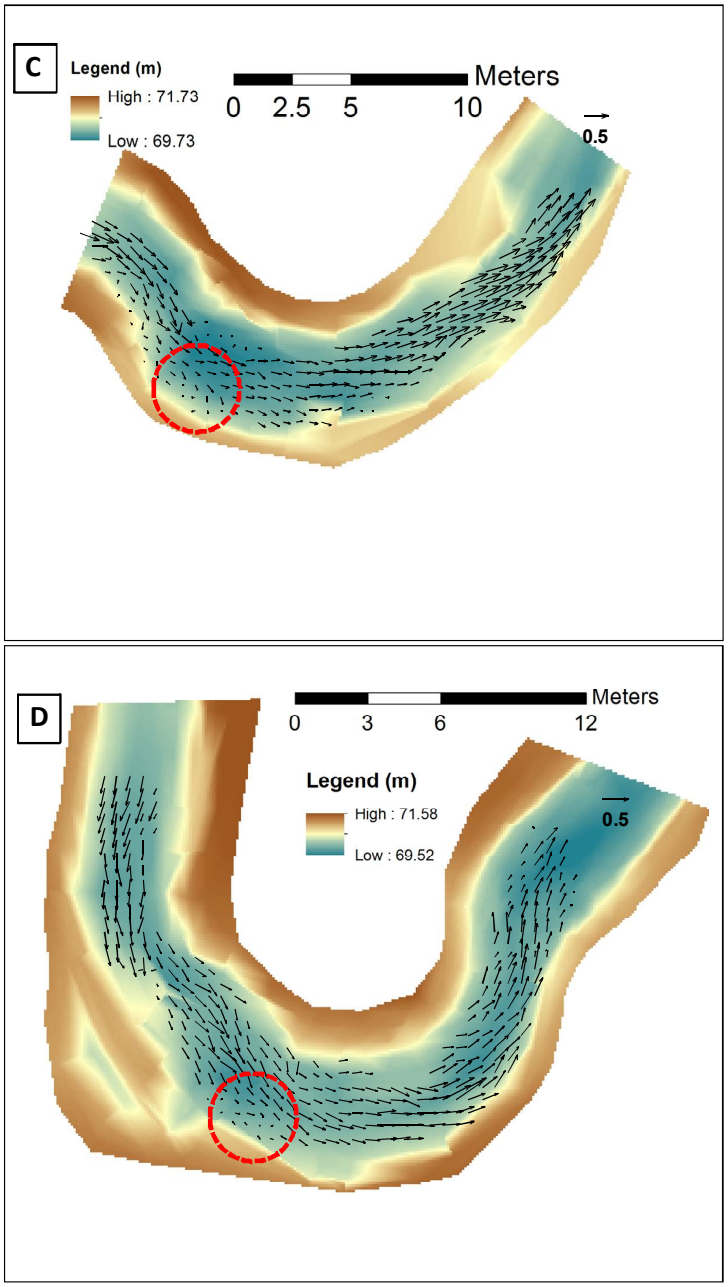

Figure 10. Measured depth-averaged ADCP velocities in the meander bends of the M4 sub-reach at: (**a**) first bend during August 2014 (low flow); (**b**) second bend during August 2014 (low flow); (**c**) fist bend during October 2014 (moderate flow); (**d**) second bend during October 2014 (moderate flow). Refer to Figure 1c for location of these bends. Surveyed bathymetric data (2014) are shown in the background. Note that the circles show the induced reverse eddies.

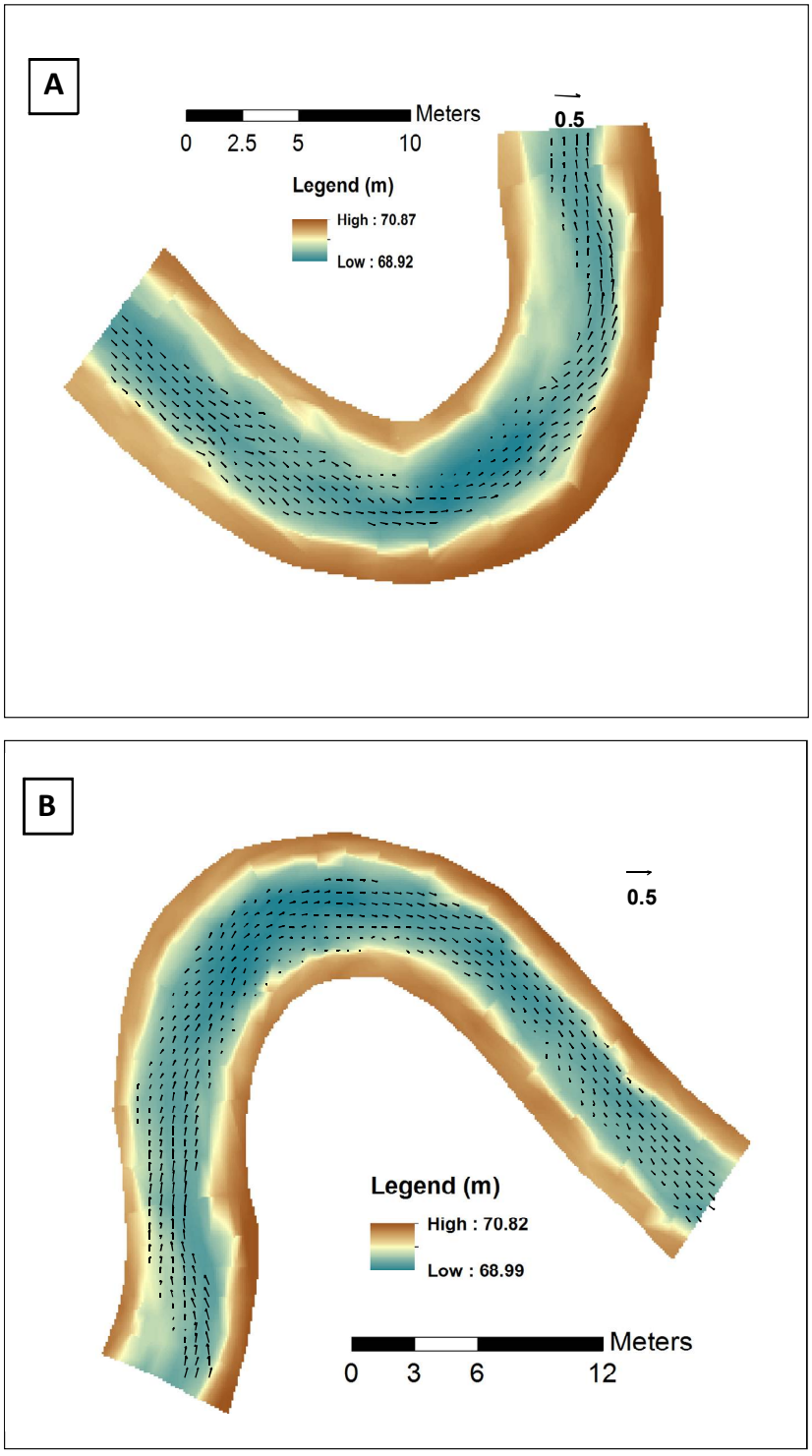

Figure 11. *Cont.*

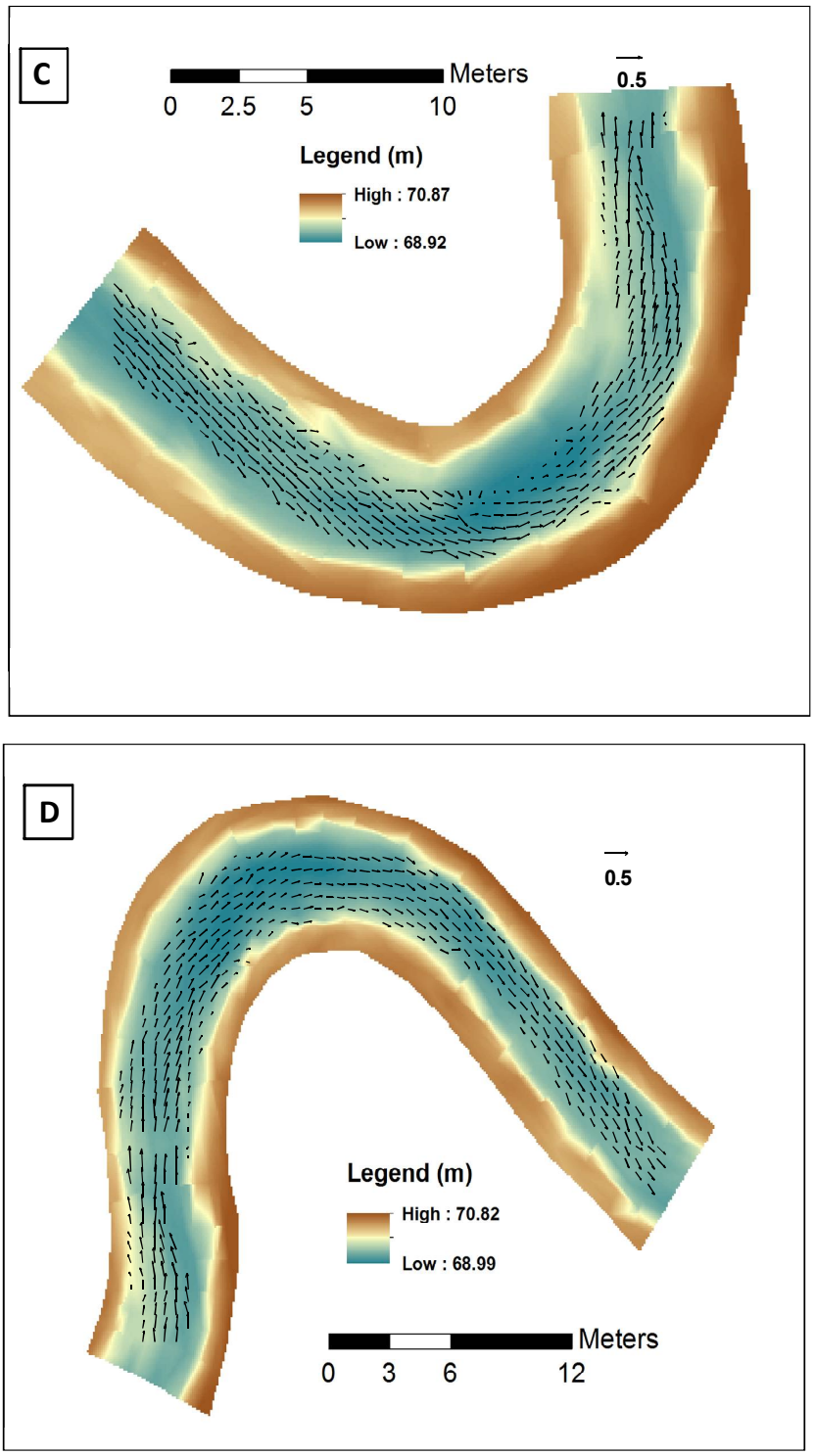

Figure 11. Measured depth-averaged ADCP velocities in the meander bends of the M3 sub-reach at: (**a**) first bend during August 2014 (low flow) (**b**) second bend during August 2014 (low flow) (**c**) fist bend during October 2014 (moderate flow) (**d**) second bend during October 2014 (moderate flow). Refer to Figure 1c for location of these bends. Surveyed bathymetric data (2014) are shown in the background.

4. Discussion

The morphology of meandering cohesive bed rivers is yet not fully understood, particularly when they are confined. The results of this study illustrated an irregular meandering pattern in the

confined sub-reach of the study creek. This irregular meandering pattern included development of a concave-bank bench in the upstream portion of outer bank in the confined sampling reach.

Page and Nanson developed a conceptual model for the formation of a concave-bank bench [40], which begins with cut-bank erosion that enlarges the channel. The possible growth of a point bar upstream of a sharp bend would deflect the flow and would leave a region of flow expansion and separation downstream and beside the upstream limb of the concave bank, which generates large eddies and induces reverse flow. The developed reverse flow causes the upstream margin of the inner bend to erode and thus widen the channel. Consequently, compensating sedimentation may occur in the downstream portion of the inner meander bend, which leads to downstream migration of the meander. The vacated zone at the upstream limb of the outer bend could be filled with eddy accretion consisting mostly of fine grains, leading to development of a concave-bank bench. In coherence with the Page and Nanson conceptual model for development of a concave-bank bench, the encroachment of the railway embankment on the M4 sampling reach in the study area confined the lateral erosion and caused the meander to migrate downstream, which provided room for fine-grained accretion on the outer meander bends. On the other hand, a lower ratio of the bedload to the suspended load in this semi-alluvial cohesive-bed river may have limited downstream development of the point bar [43,47]. This may have created an open space for separation zone and flow expansion. The measured ADCP velocities in the confined meander (Figure 10) confirmed the creation of the reverse flows caused by the flow expansion which would favor the development of the concave-bank bench. Spatially distributed ADCP velocity measurements employed in the present study provide the first corroborative proof for the theory developed by [40], which was not previously supported by detailed velocity field measurements.

Nanson and Page indicated that during the process of eddy accretion, a longitudinal-shaped bar could be developed [41], close to the concave bank and upstream of the meander apex, prior to the full formation of the bench. As a result, a secondary channel may occur since the generated longitudinal bar bench may fail to migrate completely to the concave bank. This longitudinal bar serves as a core for further deposition. Gradual deposition and aggradation of the bar leads to complete formation of the concave-bank bench. Figure 4a shows the creation of a longitudinal-shaped bar and an induced secondary channel in the confined M4 sampling reach. This can be caused by the sedimentation in the flow separation zone at the upstream of the outer bank.

Bank instability, which was mostly observed in the confined section, can be attributed to induced reverse eddy currents, which facilitate the undercut erosion and bank failure on the upstream of the outer banks. Another possible reason for the observed bank instability in the confined setting could be linked to elevated pore water pressure during flood drawdown, which cannot rapidly drain due to the cohesive nature of the bank. With a decline of the spring freshet flow stage and removal of the confining river pressure, the elevated pore water pressure could reduce the frictional shear strength and increase the unit weight of the bank material, which may have contributed to the observed bank failures. Furthermore, construction of the railway embankment may have consolidated the river bank, further hindering dissipation and drainage of elevated pore water pressures in the river bank.

5. Conclusions

Despite previous research on meander migration patterns, both the impact of channel confinement and the detailed hydro-morphodynamics in a cohesive meandering clay bed river are not yet fully understood. The present study examined the meandering behavior of a cohesive clay bed river over a 10-year period. Two sub-reaches of the same meandering cohesive clay bed river were shown to have different morphodynamic characteristics and migration pattern. The unconfined sampling reach had a typical meandering pattern with erosion on the outer banks and deposition on the inner banks of meander bends. The sinuosity of the reach remained more-or-less constant over the ten-year period. On the other hand, analysis of aerial images along with LIDAR data, total station survey, and field examination revealed an irregular meandering pattern in the confined sub-reach. The sinuosity of this

part of the creek decreased from 1.55 to 1.49. The average rate of bank retreat was 0.2 and 0.08 m/year in the confined and unconfined sub-reaches, respectively. The results showed an evolution of the concave-bank bench on the upstream limb of the outer banks of the sharp menders in the confined reach, whereas bank instability was observed downstream of the bend apices. It was shown that different locations along a river, depending on degree of channel confinement, could have distinctly different morphological characteristics. To explore how the morphodynamics of each sub-reach could be linked to its hydrodynamics, we employed spatially intensive ADCP surveying. ADCP measurements confirmed that the averaged values of the flow characteristics such as depth, velocity and Froude number were quantitatively quite similar in both sub-reach; however, the results of spatially distributed ADCP depth-averaged velocities confirmed the occurrence of reverse flow on the upstream limb of the outer meander bends in the confined sub-reach, which could be linked to the irregular meandering pattern and generation of the concave-bank bench. The results of this study shed light on the potential impacts of channel confinement on the bank retreat and river migration in comparable case studies.

Acknowledgments: The authors wish to thank Bina Chakraburtty at the National Capital Commission for project support and funding, as well as provision of the LIDAR data.

Author Contributions: Parna Parsapour-Moghaddam and Colin D. Rennie conceived and designed the study, performed the field work, analyzed the data, and wrote the paper. Parsapour-Moghaddam performed the bulk of the initial data analysis and wrote the first draft of the manuscript.

Conflicts of Interest: The authors declare no conflict of interest.

References

1. Thomson, J. On the origin of windings of rivers in alluvial plains, with remarks on the flow of water round bends in pipes. *Proc. R. Soc. Lond.* **1876**, *25*, 5–8. [CrossRef]
2. Einstein, A. The Cause of the Formation of Meanders in the Courses of Rivers and of the So-Called Baer's Law. *Die Naturwiss.* **1926**, *14*, 223–224. [CrossRef]
3. Bridge, J.S.; Jarvis, J. Flow and sedimentary processes in the meandering river South Esk, Glen Clova, Scotland. *Earth Surf. Process. Landf.* **1976**, *1*, 303–336. [CrossRef]
4. Thompson, A. Secondary flows and the pool-riffle unit: A case study of the processes of meander development. *Earth Surf. Process. Landf.* **1986**, *11*, 631–641. [CrossRef]
5. Ikeda, S.; Parker, G. (Eds.) *River Meandering*; American Geophysical Union: Washington, DC, USA, 1989.
6. Demuren, A.O. A numerical model for flow in meandering channels with natural bed topography. *Water Resour. Res.* **1993**, *29*, 1269–1277. [CrossRef]
7. Blanckaert, K.; de Vriend, H.J. Nonlinear modeling of mean flow redistribution in curved open channels. *Water Resour. Res.* **2003**, *39*. [CrossRef]
8. Lanzoni, S.; Seminara, G. On the nature of meander instability. *J. Geophys. Res. Earth Surf.* **2006**, *111*. [CrossRef]
9. Alam, J.B.; Uddin, M.; Ahmed, U.J.; Cacovean, H.; Rahman, H.M.; Banik, B.K.; Yesmin, N. Study of morphological change of river old Brahmaputra and its social impacts by remote sensing. *Geogr. Tech.* **2007**, *2*, 1–11.
10. Alam, J.B.; Uddin, M.; Ahmed, J.U.; Rahman, M.H.; Banik, B.K.; Yesmin, N.; Islam, M. Study of the morphological change of the river old Brahmaputra and its impacts. *Asian J. Water Environ. Pollut.* **2009**, *6*, 11–19.
11. Blanckaert, K. Hydrodynamic processes in sharp meander bends and their morphological implications. *J. Geophys. Res. Earth Surf.* **2011**, *116*. [CrossRef]
12. Kasvi, E.; Vaaja, M.; Alho, P.; Hyyppä, H.; Hyyppä, J.; Kaartinen, H.; Kukko, A. Morphological changes on meander point bars associated with flow structure at different discharges. *Earth Surf. Process. Landf.* **2013**, *38*, 577–590. [CrossRef]
13. Asahi, K.; Shimizu, Y.; Nelson, J.; Parker, G. Numerical simulation of river meandering with self-evolving banks. *J. Geophys. Res. Earth Surf.* **2013**, *118*, 2208–2229. [CrossRef]

14. Kasvi, E.; Vaaja, M.; Kaartinen, H.; Kukko, A.; Jaakkola, A.; Flener, C.; Hyyppä, H.; Hyyppä, J.; Alho, P. Sub-bend scale flow–sediment interaction of meander bends—A combined approach of field observations, close-range remote sensing and computational modelling. *Geomorphology* **2015**, *238*, 119–134. [CrossRef]
15. Parsapour-Moghaddam, P.; Rennie, C.D. Hydrostatic versus nonhydrostatic hydrodynamic modelling of secondary flow in a tortuously Meandering River: Application of Delft3D. *River Res. Appl.* **2017**, *33*, 1400–1410. [CrossRef]
16. Parsapour-Moghaddam, P.; Rennie, C.D. Calibration of a 3D Hydrodynamic Meandering River Model Using Fully Spatially Distributed 3D ADCP Velocity Data. *J. Hydraul. Eng.* **2018**, *144*, 04018010.
17. Schuurman, F.; Shimizu, Y.; Iwasaki, T.; Kleinhans, M.G. Dynamic meandering in response to upstream perturbations and floodplain formation. *Geomorphology* **2016**, *253*, 94–109. [CrossRef]
18. Hooke, J. River meander behaviour and instability: A framework for analysis. *Trans. Inst. Br. Geogr.* **2003**, *28*, 238–253. [CrossRef]
19. Hodskinson, A.; Ferguson, R.I. Numerical modelling of separated flow in river bends: Model testing and experimental investigation of geometric controls on the extent of flow separation at the concave bank. *Hydrol. Process.* **1998**, *12*, 1323–1338. [CrossRef]
20. Ferguson, R.I.; Parsons, D.R.; Lane, S.N.; Hardy, R.J. Flow in meander bends with recirculation at the inner bank. *Water Resour. Res.* **2003**, *39*. [CrossRef]
21. Blanckaert, K.; Kleinhans, M.G.; McLelland, S.J.; Uijttewaal, W.S.; Murphy, B.J.; van de Kruijs, A.; Parsons, D.R. Flow Separation and Morphology in Sharp Meander Bends. In Proceedings of the AGU Fall Meeting, San Francisco, CA, USA, 13–17 December 2010; American Geophysical Union: Washington, DC, USA, 2010.
22. Constantinescu, G.; Kashyap, S.; Tokyay, T.; Rennie, C.D.; Townsend, R.D. Hydrodynamic processes and sediment erosion mechanisms in an open channel bend of strong curvature with deformed bathymetry. *J. Geophys. Res. Earth Surf.* **2013**, *118*, 480–496. [CrossRef]
23. Blanckaert, K.; Kleinhans, M.G.; McLelland, S.J.; Uijttewaal, W.S.; Murphy, B.J.; Kruijs, A.; Parsons, A.; Chen, Q. Flow separation at the inner (convex) and outer (concave) banks of constant-width and widening open-channel bends. *Earth Surf. Process. Landf.* **2013**, *38*, 696–716. [CrossRef]
24. Nardi, L.; Campo, L.; Rinaldi, M. Quantification of riverbank erosion and application in risk analysis. *Nat. Hazards* **2013**, *69*, 869–887. [CrossRef]
25. Rinaldi, M.; Casagli, N.; Dapporto, S.; Gargini, A. Monitoring and modelling of pore water pressure changes and riverbank stability during flow events. *Earth Surf. Process. Landf.* **2004**, *29*, 237–254. [CrossRef]
26. Simon, A.; Collison, A.J. Pore-water pressure effects on the detachment of cohesive streambeds: Seepage forces and matric suction. *Earth Surf. Process. Landf.* **2001**, *26*, 1421–1442. [CrossRef]
27. Pizzuto, J. An empirical model of event scale cohesive bank profile evolution. *Earth Surf. Process. Landf.* **2009**, *34*, 1234–1244. [CrossRef]
28. Salem, H.; Rennie, C.D. Practical determination of critical shear in cohesive soils. *J. Hydraul. Eng. (ASCE)* **2017**, *143*, 04017045. [CrossRef]
29. Eke, E.; Parker, G.; Shimizu, Y. Numerical modeling of erosional and depositional bank processes in migrating river bends with self-formed width: Morphodynamics of bar push and bank pull. *J. Geophys. Res. Earth Surf.* **2014**, *119*, 1455–1483. [CrossRef]
30. Casagli, N.; Curini, A.; Gargini, A.; Rinaldi, M.; Simon, A. Effects of pore pressure on the stability of streambanks: Preliminary results from the Sieve River, Italy. In Proceedings of the Management of Landscapes Disturbed by Channel Incision, Oxford, MS, USA, 19–23 May 1997; pp. 243–248.
31. Simon, A.; Curini, A. Pore pressure and bank stability: The influence of matric suction. In Proceedings of the Water Resources Engineering 98, Memphis, TN, USA, 3–7 August 1998; pp. 358–363.
32. Rinaldi, M.; Casagli, N. Stability of streambanks formed in partially saturated soils and effects of negative pore water pressures: The Sieve River (Italy). *Geomorphology* **1999**, *26*, 253–277. [CrossRef]
33. Simon, A.; Curini, A.; Darby, S.E.; Langendoen, E.J. Bank and near-bank processes in an incised channel. *Geomorphology* **2000**, *35*, 193–217. [CrossRef]
34. Choné, G.; Biron, P.M. Assessing the relationship between river mobility and habitat. *River Res. Appl.* **2016**, *32*, 528–539. [CrossRef]
35. Nicoll, T.J.A. Planform Geometry and Kinematics of Confined Meandering Rivers on the Canadian Prairies. Master's Thesis, Simon Fraser University, Burnaby, BC, Canada, 2008.

36. Ghinassi, M.; Ielpi, A.; Aldinucci, M.; Fustic, M. Downstream-migrating fluvial point bars in the rock record. *Sediment. Geol.* **2016**, *334*, 66–96. [CrossRef]
37. Lewin, J.; Brindle, B.J. Confined meanders. In *River Channel Changes*; Gregory, K.J., Ed.; John Wiley and Sons: Chichester, UK, 1977; pp. 221–233.
38. Lane, E.W. *A Study of the Shape of Channels Formed by Natural Streams Flowing in Erodible material*; US Army Engineer Division, Sediment Series, 9; Mississippi River Corps of Engineers: Omaha, NE, USA, 1957.
39. Nicoll, T.J.; Hickin, E.J. Planform geometry and channel migration of confined meandering rivers on the Canadian prairies. *Geomorphology* **2010**, *116*, 37–47. [CrossRef]
40. Page, K.; Nanson, G. Concave-bank benches and associated floodplain formation. *Earth Surf. Process. Landf.* **1982**, *7*, 529–543. [CrossRef]
41. Nanson, G.C.; Page, K. Lateral accretion of fine-grained concave benches on Meandering Rivers. In *Modern and Ancient Fluvial Systems*; Collinson, J., Lewin, J., Eds.; International Association of Sedimentologists Special Publication: Gent, Belgium, 1983; Volume 6, pp. 133–143.
42. Burge, L.M.; Smith, D.G. Confined meandering river eddy accretions: sedimentology, channel geometry and depositional processes. In *Fluvial Sedimentology VI*; Smith, N.D., Rogers, J., Eds.; Special Publication of Internat, the International Association of Sedimentologists: Gent, Belgium, 1999; Volume 28, pp. 113–130.
43. Makaske, B.; Weerts, H.J. Muddy lateral accretion and low stream power in a sub-recent confined channel belt, Rhine-Meuse Delta, central Netherlands. *Sedimentology* **2005**, *52*, 651–668. [CrossRef]
44. Smith, D.G.; Hubbard, S.M.; Leckie, D.A.; Fustic, M. Counter point bar deposits: lithofacies and reservoir significance in the meandering modern Peace River and ancient McMurray Formation, Alberta, Canada. *Sedimentology* **2009**, *56*, 1655–1669. [CrossRef]
45. Daniel, J.F. *Channel Movement of Meandering Indiana Streams (No. 732)*; United States Geological Survey Professional Paper 732-A; Geological Survey: Reston, VA, USA, 1971; 18p.
46. Lewin, J. Meander development and floodplain sedimentation: A case study from mid-Wales. *Geol. J.* **1978**, *13*, 25–36. [CrossRef]
47. Jamieson, E.C.; Ruta, M.A.; Rennie, C.D.; Townsend, R.D. Monitoring stream barb performance in a semi-alluvial meandering channel: Flow field dynamics and morphology. *Ecohydrology* **2013**, *6*, 611–626. [CrossRef]
48. Maarschalk-Bliss, S. Seasonal Variation in Assemblage Structure and Movement of Small Stream Fish in an Urban Environment. Master's Thesis, Biology, Carleton University, Ottawa, ON, Canada, 2014.
49. Salem, H.; Rennie, C.D.; Custodio, C.Z. Influence of Pore Pressure on Clay Erosion. In Proceedings of the River Flow Proceedings, Lausanne, Switzerland, 3–5 September 2014.
50. Biron, P.M.; Choné, G.; Buffin-Bélanger, T.; Demers, S.; Olsen, T. Improvement of streams hydro-geomorphological assessment using LIDAR DEMs. *Earth Surf. Process. Landf.* **2013**, *38*, 1808–1821. [CrossRef]
51. De Rose, R.C.; Basher, L.R. Measurement of river bank and cliff erosion from sequential LIDAR and historical aerial photography. *Geomorphology* **2011**, *126*, 132–147. [CrossRef]
52. Williams, R.D.; Rennie, C.D.; Brasington, J.; Hicks, D.M.; Vericat, D. Linking the spatial distribution of bed load transport to morphological change during high-flow events in a shallow braided river. *J. Geophys. Res. Earth Surf.* **2015**, *120*, 604–622. [CrossRef]
53. Parsapour-moghaddam, P.; Rennie, C.D.; Midwood, J.; Cvetkovic, M.; Cooke, S.J. Influence of Channel Erosion on Fish Habitat Utilization. In Proceedings of the 36th IAHR World Congress, Hague, The Netherlands, 28 June–3 July 2015.
54. Brennan, C.P.; Parsapour-moghaddam, P.; Rennie, C.D.; Seidou, O. Continuous prediction of clay-bed stream erosion in response to climate model output for a small urban watershed. *J. Hydrol. Process.* **2018**, in press. [CrossRef]
55. Rennie, C.D.; Church, M. Mapping spatial distributions and uncertainty of water and sediment flux in a large gravel bed river reach using an acoustic Doppler current profiler. *J. Geophys. Res. Earth Surf.* **2010**, *115*, F03035. [CrossRef]

56. Parsapour-Moghaddam, P.; Rennie, C.D. ADCP Validation of 3D Morphodynamic Modelling in Clay-Bed Meandering Rivers. In Proceedings of the 36th IAHR World Congress, Hague, The Netherlands, 28 June–3 July 2015.
57. Parsapour-Moghaddam, P.; Rennie, C.D. 3D versus 2D calibration of a 3D hydrodynamic model. In Proceedings of the 37th IAHR World Congress, Kuala Lumpur, Malaysia, 13–18 August 2017.